SCANNING VOL. 37, 197–203 (2015)
© Wiley Periodicals, Inc.

# Nanostructured Vanadium Carbide Thin Films Produced by RF Magnetron Sputtering

SUAT PAT AND ŞADAN KORKMAZ

Physics Department, Eskişehir Osmangazi University, Turkey

**Summary:** In this paper, nanostructured vanadium carbide thin films were deposited on glass substrates and their optical and surface properties were analyzed. All produced samples were transparent in the optical region. Refractive index values were calculated using the Drude model. According to contact angle measurements of the coated surfaces, the samples show high wettability. The surface free energies of the samples were found to be very similar. The influence of the nitrogen content in the buffer gas mixture was determined; it was concluded that the microstructure, refractive index, surface morphology, surface free energy, and thickness of thin films can change in response to the nitrogen concentration of the radio frequency (RF) buffer gas. SCANNING 37:197–203, 2015. © 2015 Wiley Periodicals, Inc.

**Key words:** Sputtered films, XRD, AFM, XRD

## Introduction

Vanadium carbide (VC) thin films have relatively high hardness, a high melting point, good chemical stability, good electrical conductivity, and high thermal conductivity (Ferro *et al*., 2008; Aguzolli *et al*., 2012). VC coatings are used for protective hard coatings, wear protection, and friction reduction in turbine blades and cutting tools (Ferro *et al*., 2008; Portolan *et al*., 2009; Aguzolli *et al*., 2012). VC coatings also have good corrosion resistance compared with alloys (Fazluddin *et al*., '95). VC thin films show excellent properties for commercial applications (Wu *et al*., 2009).

Various methods are being used for VC coatings and thin film deposition. These methods include reactive magnetron sputtering (Ferro *et al*., 2008; Wu *et al*., 2009), DC reactive magnetron sputtering (Aguzolli *et al*., 2012; Portolan *et al*., 2009), thermal diffusion (TD, Fazluddin *et al*., '95), femtosecond pulsed laser deposition (Teghil *et al*., 2009), electron probe micro-analysis (Aouni *et al*., 2004), and hydrothermal processes (Ma *et al*., 2010).

In this paper, the influence of $N_2$ concentration on the micro-structural, optical, and surface properties of nanostructured VC thin films is presented. The parameters of RF magnetron sputter deposition affect the ion energy and impact cross-section, thus influencing grain growth, morphology and crystallographic structure (Hübler *et al*., '99; Chawla *et al*., 2008; Andres, 2010). Various N-rich some structures can be presented (Greczynski *et al*., 2010). The thin films' microstructure, phase analysis, surface composition, 2D and 3D surface images, contact angle (CA), surface free energy (SFE), transmittance and refractive index were investigated with respect to variations in $N_2$ concentration. The optical and surface properties were analyzed by field emission scanning electron microscopy (FESEM), wavelength dispersive spectroscopy (WDS), atomic force microscopy (AFM), and optical tensiometry. The optical properties were studied by UV-Vis spectrophotometry and interferometry. Determination of the refractive index was carried out using the Drude model. Four different heavy media and five calculation models were used for SFE determination. Some novel findings are presented in this paper. The $N_2$ ratio in the buffer gas was directly related to the C content in the thin-layer surface composition. CA and SFE were not strongly affected by the $N_2$ ratio. These results are good agreement with the literature which studies investigation structure zone diagram (SZDs) and high power impulse magnetron sputtering (HIPIMS) (Hübler *et al*., '99; Chawla *et al*., 2008; Andres, 2010; Greczynski *et al*., 2010).

Contract grant sponsor: ESOGU; Contract grant number: BAP201219026 and 201319D23.

*Address for reprints: Suat PAT, Physics Department, Eskişehir Osmangazi University, 26480, Turkey.
E-mail: suatpat@ogu.edu.tr

Received 3 November 2014; revised 28 January 2015; Accepted with revision 3 February 2015

DOI: 10.1002/sca.21199
Published online 30 March 2015 in Wiley Online Library (wileyonlinelibrary.com).

TABLE I RF magnetron sputtering parameters

| Sample ID | Ar (%) | $N_2$ (%) | Pressure (mTorr) | Applied Power | Time |
|---|---|---|---|---|---|
| N | 10 | 90 | $4 \times 10^{-1}$ | 300 W | 70 mins |
| O | 50 | 50 | $4 \times 10^{-1}$ | 300 W | 70 mins |
| P | 70 | 30 | $4 \times 10^{-1}$ | 300 W | 70 mins |

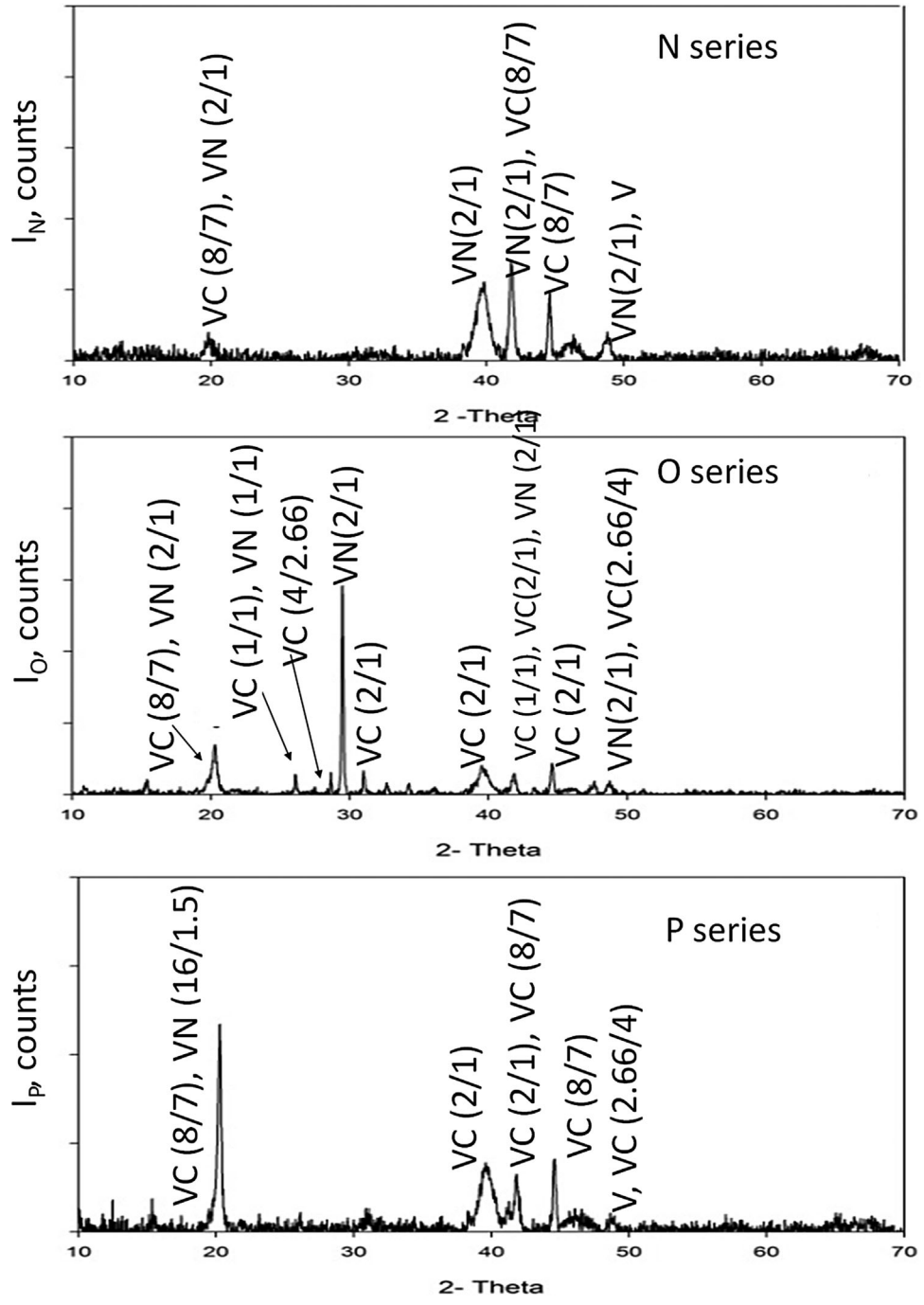



Fig. 1. XRD patterns of nanostructured VC thin films.

## Experimental Setup

VC thin films were deposited on glass substrates for optical property analysis by RF reactive magnetron sputtering using an Ar-$N_2$ gas mixture. The target used was a high purity 2-inch VC disc. The Ar:$N_2$ composition rate was adjusted to ratios of 1:9, 1:1 and 7:3. Other parameters such as working pressure, applied power, time, and sample holder position were held constant. The deposition parameters are summarized in Table I.

A PANalytical Empyrean XRD instrument was used to determine the microstructure and crystallographic properties of nanostructured VC thin films. Two-dimensional surface topography imaging of the nanostructured VC layers was performed using ultra high resolution field emission scanning electron microscopy (FESEM, Carl Zeiss Supra 40 VP). For surface composition analysis, wavelength dispersive and energy dispersive spectrometry (WDS) was used. All samples were coated by DC sputtering before the imaging procedures. Ambios Q-Scope atomic force microscopy was used for 3D imaging and roughness measurements. An Attension Theta Lite optical tensiometer was used to measure CA and surface free energy. For these measurements, four heavy media and five theoretical methods were used. Transmittance spectra were collected using a UV–Vis double beam spectrophotometer. Refractive index measurements were collected using a Filmetrics F20 interferometer.

## Results and Discussion

The thicknesses of the deposited films were measured using a Filmetrics F20 interferometer, yielding values of approximately 60 nm for the N series, 140 nm for the O series, and 150 nm for the P series. According to the Drude model, the refractive indices of the N, O, and P samples were 1.50, 1.62, and 1.57, respectively, at 632 nm.

The XRD patterns of the produced thin films are shown in Figure 1. The obtained crystallographic data are summarized in Table II. Vanadium carbide and vanadium nitride phases are visible in the XRD data. Furthermore, vanadium atoms are linked to nitrogen atoms. The calculated reaction ratios are related to the composition of the buffer gas. Vanadium carbide has a hexagonal crystal structure.

Because the investigated substrate is an amorphous material, the obtained peaks represent the coated layers. The full width at half maximum (FWHM) of observed peaks is an important metric for calculating grain size. The Debye-Scherer equation gives the average crystalline size (Xu *et al*., 2000; Pat *et al*., 2011; Vinila *et al*., 2014). Using the Debye–Scherer equation, the average grain sizes can be calculated as approximately 27 nm for the N series, 50 nm for the O series, and 40 nm for the P series. Crystalline sizes smaller than 50 nm are characteristic of nanocrystalline materials. These findings are consistent with the results of FESEM and AFM imaging.

According to Table II, the $N_2$ concentration in the buffer gas plays an important role in the crystallographic structure of the samples. In Table II, references number is the database spectrum IDs number which retrieved from database library. A score is calculated for all candidates to determine how well they match the experimental data. A high score indicates a better match to experimental data. All three XRD spectra indicate polycrystalline form. Differences in composition can be attributed to the differences in nitrogen concentration.

Surface topography measurements of the surface layer were realized using field emission scanning electron microscopy (FESEM) and atomic force microscopy (AFM). FESEM and AFM images are illustrated in Figure 2. Images (a) and (c) were taken at 150,000× magnification. Image (d) was taken at 200,000×

TABLE II XRD peak list

| Samples ID | References number | Compound name | Chemical Formula | Score |
|---|---|---|---|---|
| | 98-007-7564 | Vanadium Carbide | C1 V2 | 39 |
| | 98-004-1504 | Vanadium | V1 | 68 |
| N | 98-008-5953 | Vanadium Carbide | C7 V8 | 13 |
| | 98-000-8236 | Vanadium Nitride | N1 V2 | 32 |
| | 98-004-2746 | Vanadium Carbide | C2.66 V4 | 6 |
| | 98-000-8236 | Vanadium Nitride | N1 V2 | 15 |
| O | 98-002-6949 | Vanadium(III) Nitride | N1 V1 | 22 |
| | 98-002-6953 | Vanadium (IV) Carbide | C1 V1 | 22 |
| | 98-010-8192 | Vanadium Carbide | C1 V2 | 12 |
| | 98-004-1504 | Vanadium | V1 | 47 |
| | 98-008-6370 | Vanadium Nitride | N1.5 V16 | 12 |
| P | 98-007-7564 | Vanadium Carbide | C1 V2 | 27 |
| | 98-008-5953 | Vanadium Carbide | C7 V8 | 12 |
| | 98-004-2746 | Vanadium Carbide | C2.66 V4 | 7 |

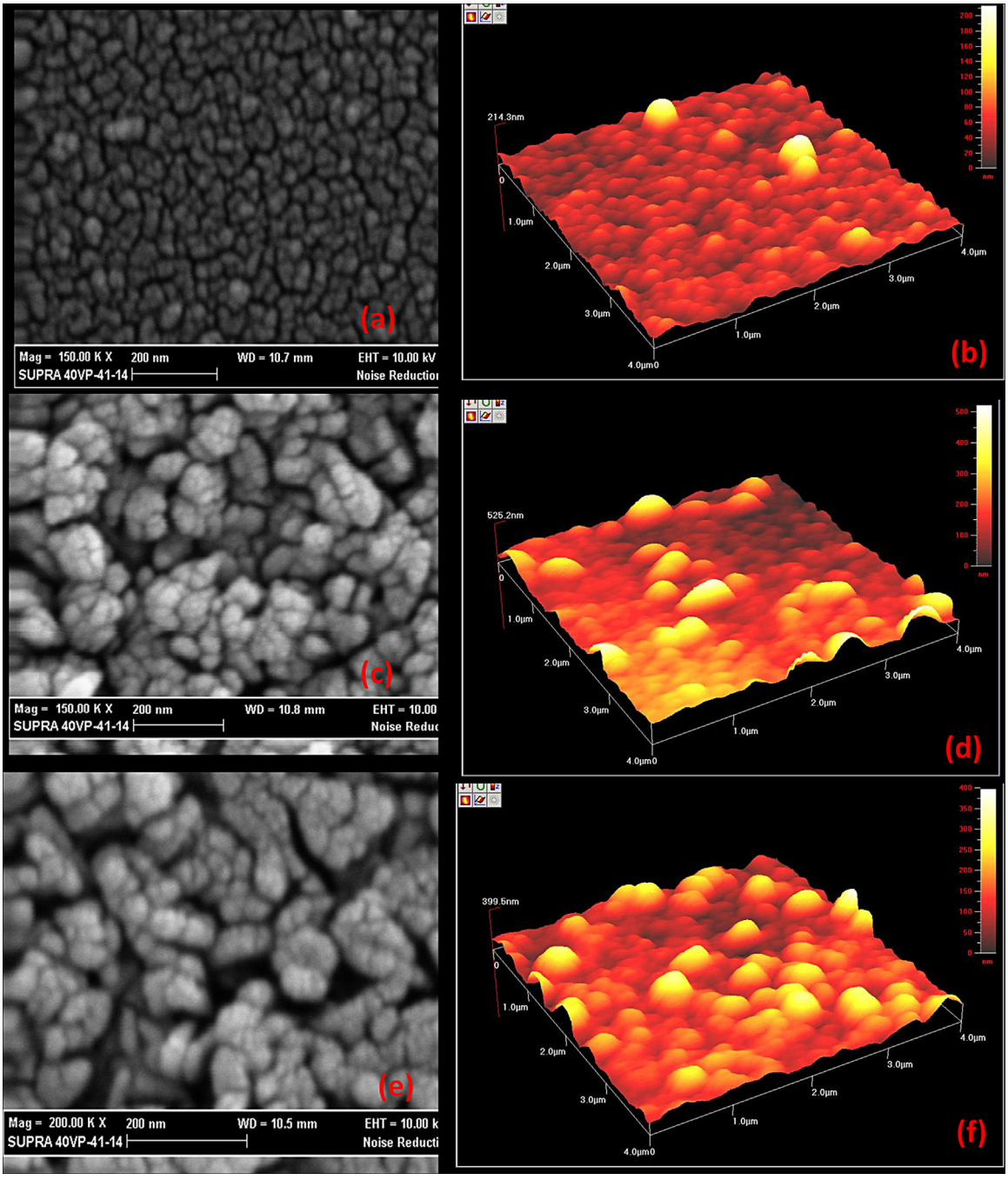



Fig. 2. FESEM and AFM images of sample N (a and b), O (c and d) and P (e and f).

magnification. As the FESEM images show, image (a) is different from the others. These differences are related to the nitrogen percentage. In particular, the N series (Fig. 2a) has a much smaller particle size than the other series. The obtained FESEM images are fairly similar to images presented in the literature (Zhang and Li, 2005; Hossein-Zadeh and Mirzaee, 2014; Kurlov and Gusev, 2013; Hossein-Zadeh *et al*., 2014). All AFM images were collected at a $4 \times 4$ μm scale. FESEM and AFM images were obtained at approximately the same scale, and the resulting images are similar. The average roughness values were determined to be 14, 53, and 41 nm, respectively, using 40 line measurements at this scale. The values calculated from the Debye–Scherer equation were confirmed by the FESEM and AFM images. For all samples, the entire surface was homogenous and nano-structured.

As Figure 2a and b clearly show, grains are randomly distributed with similar sizes and shapes. The approximate grain size increased with increasing of $N_2$ concentration. Wavelength-dispersive X-ray spectroscopy (WDS) was used for elemental analysis of the VC layers. The obtained

TABLE III WDS elemental analysis results

| Sample ID | Element | Wt % | Atomic % |
|---|---|---|---|
| N | Vanadium | 93.28 | 76.58 |
| | Carbide | 1.26 | 23.42 |
| O | Vanadium | 90.3 | 68.71 |
| | Carbide | 7.7 | 31.29 |
| P | Vanadium | 88.23 | 63.86 |
| | Carbide | 11.77 | 36.14 |

results are summarized in Table III. As the nitrogen content of the Ar-$N_2$ gas mixture was decreased, the carbide percentage of the coated layer increased. The results of WDS were verified using the XRD peak list.

Surface free energy (SFE) represents the surface tension of solid samples. For the determination of SFE, an optical tensiometer was used. The optical tensiometer was used to measure the surface CA. CA is directly related to SFE and surface roughness. For the calculation of the SFE, four different heavy media were used. Contact angle measurements were collected for water, ethylene glycol, formamide and di-iodomethane. SFE values were calculated using five theoretical models. CA and SFE values are given in Table IV. The obtained CA values are much lower than 90°. It is concluded that the surfaces show good hydrophilic properties.

The optical transmittance spectra of the produced thin films were determined in the wavelength range between 300 and 1100 nm using a Unico 4802 UV–Vis spectrophotometer. The obtained films are highly transparent throughout most of the visible and infrared regions. As Figure 3a shows, changes in the reactive gas composition are related to changes in the samples' transparency ratios. All samples show similar properties. The measured transparency ratios are summarized in Figure 3a.

Refractive index values are related to microstructure properties and compact structure. Calculated refractive index values are shown in Figure 3b. These data were obtained using the Drude model.

The parameters of RF magnetron sputter deposition affect the ion energy and impact cross section, thus influencing grain growth, morphology, crystallographic structure, etc. (Hübler *et al*., '99; Chawla *et al*., 2008; Andres, 2010). Various N-rich structures have been published (Greczynski *et al*., 2010). Changes in sputtering pressure can change the kinetic effect of sputtered particles during film growth. At relatively low pressure, the impact cross section is very low; hence, few collisions occur. To increase collision frequency, the sputter parameters must be changed. Ion energies are different when using high pressure sputter deposition. Positive nitrogen ions from the $N_2$ in the reactive gas arrive at the film surface. Our results show that the $N_2$ ratio in the buffer gas is directly related to the C content in the thin film surface composition. CA and SFE are not changed strongly by the $N_2$ ratio, but the thin film's micro-structural properties are strongly affected. Multiple crystal phases of growth structure were detected upon increasing the nitrogen content to an Ar/$N_2$ ratio of 1:1. These results are in good agreement with the literature which studies investigating structure zone

TABLE IV Contact angles and SFE values

| Sample ID | Heavy media | CA (°) | Method | SFE γ (N/m) |
|---|---|---|---|---|
| N | Water | 50 | Acid-base | 50 |
| | Ethylene glycol | 24 | Equation of state | 48 |
| | Formamide | 19 | Owrk/fowkes | 53 |
| | di-Iodomethane | 46 | Wu | 56 |
| | | | Zisman | 30 |
| O | Water | 43 | Acid-base | 44 |
| | Ethylene glycol | 35 | Equation of state | 49 |
| | Formamide | 33 | Owrk/fowkes | 54 |
| | di-Iodomethane | 24 | Wu | 57 |
| | | | Zisman | 25 |
| P | Water | 41 | Acid-base | 52 |
| | Ethylene glycol | 26 | Equation of state | 52 |
| | Formamide | 15 | Owrk/fowkes | 58 |
| | di-Iodomethane | 21 | Wu | 62 |
| | | | Zisman | 40 |

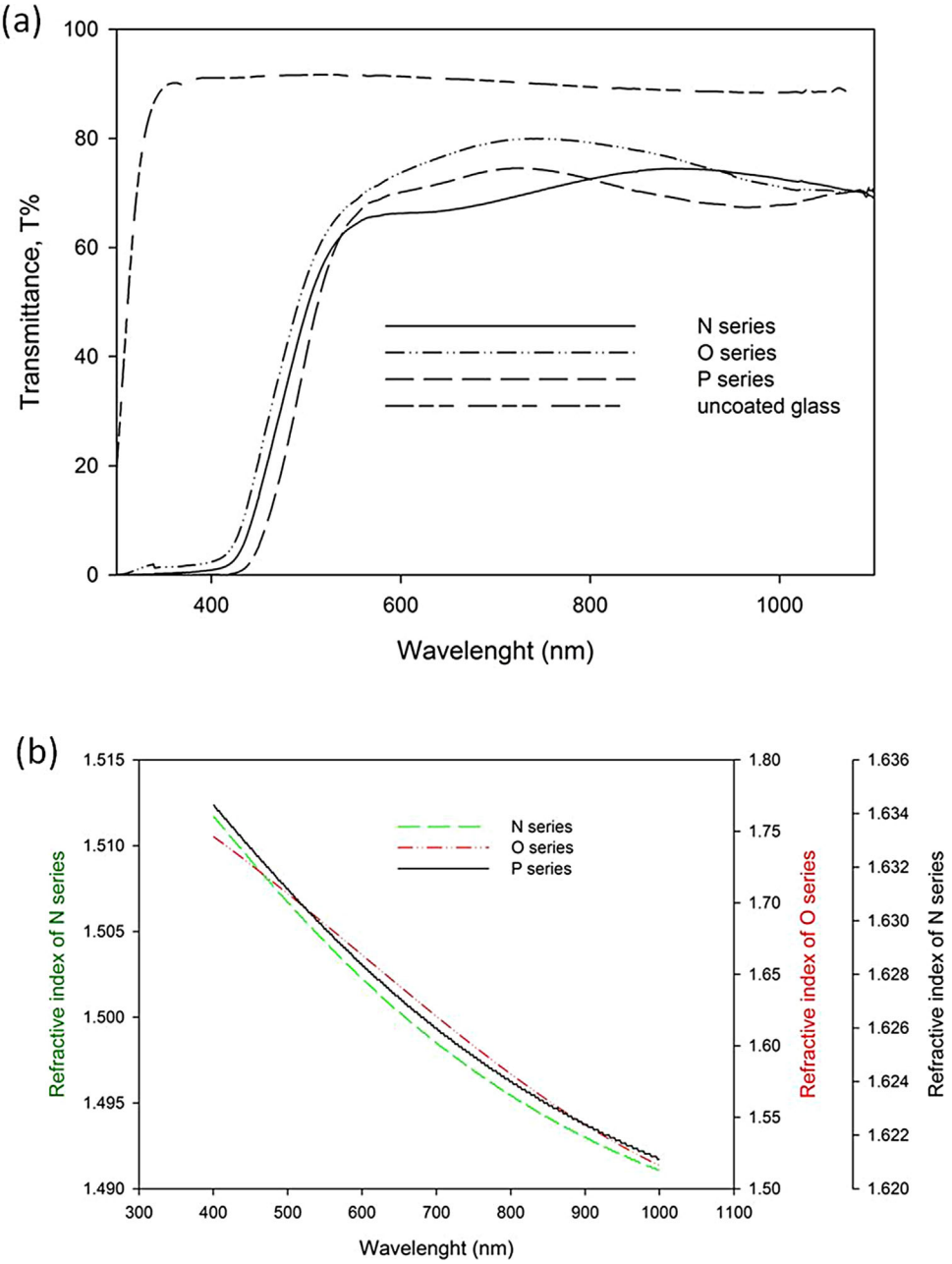



Fig. 3. (a) Transmittance and (b) refractive index values of nanostructured VC films.

diagram (SZD) and HIPIMS (Hübler *et al*., '99; Chawla *et al*., 2008; Andres, 2010; Greczynski *et al*., 2010).

## Conclusion

Nano-structured vanadium carbide (VC) thin films were deposited on glass substrates by RF magnetron sputtering. In this study, the reactive gas concentration was selected as the variable parameter. The deposited layers were characterized by various analysis techniques. The obtained results show that variations in the reactive gas composition caused changes in the optical, microstructure and morphological properties of the resulting thin films. Our results show that the $N_2$ ratio in the buffer gas is directly related to the C content in the surface layer. The crystal structure of the growth layer is related to the ion energy. Furthermore, the surface morphology and optical properties were affected by the nitrogen gas concentration. The obtained films presented polycrystalline structures. The calculated average crystalline sizes were approximately 27 nm for the N series, 50 nm for the O series, and 40 nm for the P series. FESEM and AFM images show that the grain shape is characterized by cylindrical aggregates; hence, vanadium carbide is a natural lubricant material. Contact angle values were less than 90°; hence, the investigated samples show good hydrophilic properties. The optical

properties of the films were measured using the Drude model. These determined values are comparable to characteristic values in the literature. In particular, the values of the refractive indices were approximately equal for all samples. We believe that our results are useful for quality testing of VC coatings.

## References


Aguzolli C, Figueroa CA, de Souza FS, Spinelli A, Baumvol IJR. 2012. Corrosion and nanomechanical properties of vanadium carbide thin film coatings of tool steel. Surf Coat Tech 206: 2725–2731.

Andres A. 2010. A structure zone diagram including plasma-based değposition and ion etching. Thin Solid Films 518: 4087–4090.

Aouni A, Weisbecker P, Loi TH, Bauer-Grosse E. 2004. Search for new materials in sputtered V1-xCx films. Thin Solid Films 469: 315–321.

Chawla V, Jayaganthan R, Chadra R. 2008. Structural characterization of magnetron sputtered nanocrystalline TiN thin films. 59: 1015–1020.

Fazluddin SB, Koursaris A, Ringas C, Cowie K. 1995. Mater Manuf Process 10: 159.

Ferro D, Rau JV, Generosi A, Albertini VR, Latini A, Barinov SM. 2008. Electron beam deposited VC and NbC thin films on titanium: Hardness and energy-dispersive X-ray diffraction study. Surf Coat Tech 202: 2162–2168.

Greczynski G, Jensen J, Böhlmark J, Hultman L. 2010. Microstructure control of CrNx films during high power impulse magnetron sputtering. 205: 118–130.

Hossein-Zadeh M, Mirzaee O. 2014. Synthesis and characterization of V8C7 nanocrystalline powder by heating milled mixture of V2O5, C and Ca via mechanochemical activation. Adv Powder Technol 25: 978–982.

Hossein-Zadeh M, Razavi M, SAfa M Abdollahi A, Mirzaee O. 2014. J King Saud Univ - Eng Sci (in press). dx.doi.org/10.1016/j.jksues.2014.03.010

Hübler R, Tentardini EK, Blando E, et al. 1999. The energy dependence on microstructure of (Ti-Al-V) nitrides deposited by dual ion beam sputtering. Surf Coat Tech 116–119: 969–972.

Kurlov AS, Gusev AI. 2013. Preparation and microstructure of VC0.875 nanopowder. Inorg Mater 49: 347–354.

Ma SF, Liang J, Zhao JF, Xu BS. 2010. Synthesis, characterization and growth mechanism of flower-like vanadium carbide hierarchical nanocrystals. CrystEngComm 12: 750–754.

Pat S, Temel S, Ekem N, Korkmaz S, Ozkan M, Balbag MZ. 2011. Diamond-like carbon coated on polyethylene terephthalate by Thermionic Vacuum Arc. J Plast Film Sheet 27: 127–137.

Portolan E, Amorim CLG, Soares GV, et al. 2009. Carbon occupancy of interstitial sites in vanadium carbide films deposited by direct current reactive magnetron sputtering. Thin Solid Films 517: 6493–6496.

Teghil R, De Bonis A, Galasso A, et al. 2009. Nanostructured thin films obtained by ultra-short pulse laser deposition of vanadium carbide. Appl Surf Sci 255: 5220–5223.

Vinila VS, Jacob R, Mony A, et al. 2014. XRD studies on nano crystalline ceramic superconductor PbSrCaCuO at different treating temperatures. Cryst Struct Theor Appl 3: 1.

Wu XY, Li GZ, Chen YH, Li GY. 2009. Microstructure and mechanical properties of vanadium carbide coatings synthesized by reactive magnetron sputtering. Int J Refract Met H 27: 611–614.

Xu JQ, Pan QY, Shun YA, Tian ZZ. 2000. Grain size control and gas sensing properties of ZnO gas sensor. Sensor Actuat B-Chem 66: 277–279.

Zhang B, Li ZQ. 2005. Synthesis of vanadium carbide by mechanical alloying. J Alloy Compd 392: 183–186.